Scilight

Environmental Change and Disease Dynamics

https://www.sciltp.com/journals/ecdd

Article

Development and Evaluation of a Dengue Meteorological Risk Index (DMRI) in Southern China

Jianxiong Hu [1,2,†], Liling Lin [3,†], Honglong Chen [2], Qimin Fang [2], Di Wu [2], Guanhao He [2], Tao Liu [2,4], Fangfang Zeng [2], Fengrui Jing [2], Ziqing Lin [2], Fanna Liu [1], Xiaofeng Liang [2,3], Min Kang [3,*] and Wenjun Ma [1,2,4,*]

[1] Nephrology Department, The First Affiliated Hospital, Jinan University, Guangzhou 510632, China
[2] Department of Public Health and Preventive Medicine, School of Medicine, Jinan University, Guangzhou 510632, China
[3] Guangdong Provincial Center for Disease Control and Prevention, Guangzhou 511430, China
[4] Key Laboratory of Viral Pathogenesis & Infection Prevention and Control (Jinan University), Ministry of Education, Guangzhou 510632, China
* Correspondence: kangmin@yeah.net (M.K.); mawj@gdiph.org.cn (W.M.)
† These authors contributed equally to this work.

How To Cite: Hu, J.; Lin, L.; Chen, H. et al. Development and Evaluation of a Dengue Meteorological Risk Index (DMRI) in Southern China. *Environmental Change and Disease Dynamics* **2026**, *1*(1), 5.

Received: 12 March 2026
Revised: 22 April 2026
Accepted: 11 June 206
Published: 23 June 2026

Abstract: Background: Dengue fever remains a critical public health challenge in Southern China, with outbreaks heavily driven by climatic conditions. To facilitate climate-informed early warning, this study aimed to develop and validate a Dengue Meteorological Risk Index (DMRI). Methods: Dengue surveillance records and ERA5-Land meteorological reanalysis data were collected from the six cities with the highest cumulative dengue incidence in Guangdong Province, Southern China. Using the training dataset (2016–2019), Generalized Additive Mixed Models (GAMMs) were employed to quantify the non-linear exposure-response relationships between dengue incidence and key meteorological drivers, including temperature, relative humidity, and temporal dynamics. Subsequently, a Random Forest model was utilized to estimate the relative importance of each variable. The DMRI was then formulated by integrating these relationships and weighted components, stratified into early warning tiers, and externally validated using the 2015 dataset. Results: GAMM analyses revealed an inverted U-shaped association between temperature and dengue risk, while relative humidity exhibited a positive association. Random Forest modeling identified temperature and relative humidity as the primary drivers, slightly outweighing the temporal factor. The formulated DMRI demonstrated a significant positive linear correlation with actual disease risk. External validation confirmed robust discriminative capacity across risk tiers, with weekly case counts in high-risk tiers being significantly elevated compared to low-risk tiers. Conclusions: Based on ecological associations, the developed DMRI serves as an accessible tool that translates complex meteorological and temporal drivers into actionable risk tiers within the study area. Rather than a standalone forecasting tool, it serves as a supplementary indicator that may support health authorities in early warning and inform public prevention efforts.

Keywords: dengue fever; temperature; relative humidity; risk index; early warning

1. Introduction

Dengue fever is an acute mosquito-borne infectious disease caused by the dengue virus (DENV) and transmitted primarily through the bites of Aedes mosquitoes, notably *Aedes aegypti* and *Aedes albopictus* [1]. Widely recognized as the fastest-spreading mosquito-borne viral disease, dengue yields an estimated global

incidence of 390 million infections annually [2]. Driven by global warming, rapid urbanization, and increased international mobility, the geographic footprint of dengue is continuously expanding, posing a formidable public health challenge worldwide [3,4]. In China, the burden of dengue has escalated significantly over the past two decades, with Southern China bearing the brunt of the epidemics. Situated in the subtropical monsoon climate zone, Guangdong Province features a warm and humid climate alongside abundant mosquito populations and extended vector activity periods [5,6]. Furthermore, as China's most populous province and a major hub for international trade and travel bordering Southeast Asia, Guangdong presents a complex socio-ecological environment highly susceptible to dengue transmission [6].

Meteorological conditions are considered one of the primary drivers of the spatiotemporal dynamics of dengue transmission. For example, variables such as temperature, relative humidity, and precipitation can influence the growth and development, reproductive capacity, survival, and blood-feeding behavior of *Aedes* mosquitoes, thereby affecting the efficiency of dengue virus transmission [7–9]. In addition, previous studies have shown that suitable temperature and humidity conditions may accelerate dengue virus replication within *Aedes* mosquitoes, shorten the extrinsic incubation period, and thereby enhance viral transmissibility [10,11]. This suggests that dengue transmission risk differs markedly under varying meteorological conditions. Therefore, developing dengue risk early warning tools based on meteorological factors is of great importance for the precise prevention and control of outbreaks.

Despite this well-recognized potential, translating meteorological drivers into routine public health practice remains hindered by several methodological and practical bottlenecks. On one hand, while advanced epidemiological frameworks, such as Distributed Lag Non-linear Model (DLNM) [12], are powerful in capturing complex exposure-response associations, their mathematical complexity often limits their translation into routine public health practice. On the other hand, although comprehensive risk assessment systems for dengue do exist, they typically demand multi-dimensional data inputs, including socioeconomic indicators, human mobility, and real-time vector surveillance [13]. This extensive data dependency significantly delays rapid assessment and is detrimental to timely risk communication during critical pre-outbreak windows. As a result, meteorological factors are rarely synthesized into actionable, rapid risk communication metrics for dengue, despite successful preliminary applications in non-communicable diseases, such as the community-based weather-health risk index developed by Li et al. [14]. Therefore, there is an urgent need to develop an operational early warning tool that balances epidemiological rigor with practical simplicity.

To bridge this research gap, this study aims to construct and validate a novel Dengue Meteorological Risk Index (DMRI) tailored for southern China. Drawing on comprehensive epidemiological and meteorological data from six key cities in Guangdong Province (2015–2019), we synergized Generalized Additive Mixed Models (GAMMs) and Random Forest algorithms to develop a heuristic and operational Dengue Meteorological Risk Index based on temperature, humidity, and seasonality. This index intuitively reflects the risk of dengue occurrence under varying weather conditions, thereby providing a robust scientific basis for risk communication, early warning systems, resource allocation, and the formulation of evidence-based prevention and control strategies.

2. Materials and Methods

2.1. Data Sources

Dengue case data were obtained from the Notifiable Infectious Diseases Surveillance System of the Guangdong Provincial Center for Disease Control and Prevention. The dataset comprised weekly counts of both local and imported dengue cases across 21 prefectural-level cities from 2015 to 2019, aggregated by the date of illness onset. To ensure adequate statistical power and epidemiological representativeness for subsequent modeling, this study purposively selected the top six cities with the highest cumulative case counts: Guangzhou, Chaozhou, Foshan, Shantou, Zhanjiang, and Shenzhen. These six cities accounted for 77.23% of the total reported cases in the province during the study period (Table S1). The spatial distribution of dengue cases was illustrated in Figure S1. Data from 2016 to 2019 were utilized as the training set for model construction, while the 2015 data were reserved as an independent dataset for external validation.

Based on existing epidemiological evidence and biological plausibility, this study focused on crucial meteorological determinants driving dengue transmission, specifically ambient temperature and relative humidity [8,15]. Hourly meteorological data with a spatial resolution of 0.1° × 0.1° (approximately 10 km × 10 km) were obtained from the ERA5-Land reanalysis dataset, provided by the European Centre for Medium-Range Weather Forecasts (ECMWF) [16]. Using Geographic Information System (GIS) techniques, grid-level data corresponding to the administrative boundaries of the selected cities were extracted to calculate weekly regional averages as

meteorological exposure metrics. Relative humidity was mathematically derived from ambient temperature and dew point temperature using the Magnus formula [17].

2.2. Estimation of the Exposure-Response Associations of Weather Variables and Seasonality with Dengue Incidence

Prior to model construction, multicollinearity between the meteorological predictors (temperature and relative humidity) was assessed using Pearson correlation analysis and Variance Inflation Factors (VIF). Variables were confirmed to be free of severe multicollinearity ($r < 0.7$ and $VIF < 3$, Tables S2 and S3). Given the non-linear associations between meteorological factors and infectious disease dynamics, we applied Generalized Additive Mixed Models (GAMMs) to estimate the exposure-response relationships between weather variables and dengue incidence. GAMMs uniquely combine the flexibility of Generalized Additive Models (GAMs) in fitting non-linear smoothed relationships with the capability of mixed models in handling random effects arising from hierarchical data structures, thereby effectively adjusting for spatial heterogeneity across cities [18]. Weekly dengue case counts were modeled as the response variable, assuming a quasi-Poisson distribution to account for overdispersion. Weekly scale mitigates the noise and reporting delays (e.g., weekend effects) often present in daily data, while remaining sufficiently fine-grained to capture intra-annual seasonal dynamics. The core model was formulated as follows:

$$\log\left[E(Y_{i,t})\right] = \alpha + s(Tm_{i,t}, df) + s(Rh_{i,t}, df) + s(time_t, df) + Year_t + \mu_i \quad (1)$$

where $E(Y_{i,t})$ represents the expected number of dengue cases in city i during week t; α is the intercept; $Tm_{i,t}$ and $Rh_{i,t}$ denote the mean temperature and relative humidity, respectively. To account for the delayed biological effects of weather on mosquito life cycles and viral replication, including mosquito development (1–2 weeks), viral extrinsic incubation in mosquitoes (8–12 days), intrinsic incubation in humans (4–10 days), and the sustained transmission during a mosquito's infectious lifespan, we utilized a 0–6 weeks moving average (Lag 0–6) as the exposure indicator, consistent with previous study [19]. $time_t$ represents the week of the year to control for intra-annual seasonality, while the categorical variable $Year_t$ controls for long-term inter-annual trends. μ_i denotes the city-level random effect. The function $s()$ indicates a penalized smoothing spline, and df represents the degrees of freedom. Model fit criteria and optimal specifications were evaluated by minimizing the Akaike Information Criterion (AIC). Based on the minimum AIC, the df for temperature and relative humidity were both set to 3, and for the $time$ variable, it was set to 7 per year. Model diagnostics were performed to inspect residual distributions and ensure sufficient basis dimensions for the smoothing splines, thereby preventing over-fitting or under-fitting. To facilitate the precise construction of the DMRI, we extracted the exposure-response relationships of temperature, relative humidity, and the week of the year with dengue incidence risk.

2.3. Feature Weight Determination Based on Random Forest Algorithms

To quantitatively evaluate the relative contribution of each meteorological and seasonality predictor to dengue risk, a Random Forest regression model was constructed. Weekly dengue incidence served as the dependent variable, while the Lag 0–6 moving averages of temperature and relative humidity, along with the week of the year, were incorporated as independent variables. The "Increase in Node Purity" (IncNodePurity) was employed as the metric for feature importance. This metric measures the reduction in the residual sum of squares (RSS) when a specific variable is used as a splitting node; a higher IncNodePurity value signifies a greater contribution to model performance [20]. Ultimately, the relative weight of each variable was determined by calculating the proportion of its IncNodePurity relative to the sum of all variables. We utilized RF variable importance not as strict causal estimates, but as a pragmatic, heuristic weighting scheme to construct the data-driven DMRI.

2.4. Construction of the Dengue Meteorological Risk Index (DMRI)

Based on the exposure-response curves derived from the GAMMs, relative risk values corresponding to specific values of Lag 0–6 temperature, relative humidity, and the week of the year were extracted. These risk values were then integrated with their respective Random Forest-derived weights to calculate a cumulative risk score:

$$cumrisk_t = tm.risk_t \times tm.w + rh.risk_t \times rh.w + week.risk_t \times week.w \quad (2)$$

where $cumrisk_t$ is the cumulative risk value at week t; $tm.risk_t$, $rh.risk_t$, and $week.risk_t$ are the risk values derived from the GAMM curves for temperature, relative humidity, and seasonality at week t, respectively. The terms $tm.w$, $rh.w$, and $week.w$ represent their corresponding weights generated by the Random Forest model.

To facilitate intuitive public health application and risk communication, the cumulative risk scores were standardized into a 0–100 scale using the min-max normalization method, forming the final Dengue Meteorological Risk Index (DMRI):

$$DMRI = \frac{cumrisk - \min(cumrisk)}{\max(cumrisk) - \min(cumrisk)} \times 100 \quad (3)$$

2.5. Validation and Risk Stratification of the DMRI

To validate the capability of the DMRI in characterizing dengue risk, we fitted an additional GAMM against weekly dengue case counts to quantify the exposure-response relationship. The model was formulated as follows:

$$\log[E(Y_{i,t})] = \alpha + s(DMRI_{i,t}, df) + Year_t + \mu_i \quad (4)$$

where $DMRI_{i,t}$ denotes the DMRI in city i during week t, and other notations are consistent with those in Equation (1).

Subsequently, to operationalize the DMRI for practical epidemic risk assessment, we categorized the continuous index into four distinct tiers based on its frequency distribution, utilizing the mean-standard deviation (M − SD) thresholding method [21,22]. These comprised Low (<M − 0.5 SD), Moderate (M − 0.5 SD to M + 0.5 SD), Moderately High (M + 0.5 SD to M + 1.0 SD), and High (>M + 1.0 SD) risk categories. Finally, the practical validity of this stratification scheme was evaluated by comparing the average case burden and the frequency of at-risk weeks within each stratum across both the training set (2016–2019) and the independent validation set (2015).

2.6. Sensitivity Analysis

To test the robustness of our main findings, several sensitivity analyses were conducted: (1) modifying the degrees of freedom (df) for meteorological variables in the baseline GAMM from 3 to 6; (2) adjusting the df for the time variable from 5 to 7; (3) varying the df for the DMRI in the final association GAMM from 3 to 6; (4) altering the moving average lag periods for temperature and relative humidity to Lag 0–5, Lag 0–6, and Lag 0–7 weeks; and (5) comparing the marginal and conditional R-squared (R_m^2, R_c^2) of the RF-weighted DMRI against an alternative equal-weight DMRI to evaluate the robustness of this data-driven scheme.

All statistical analyses and visualizations were performed using R software (version 4.1.1). The *mgcv* and *randomForest* packages were employed to fit the models and extract feature weights, respectively. A two-sided $p < 0.05$ was considered statistically significant.

3. Results

3.1. Descriptive Statistics of Dengue Cases and Meteorological Factors in Six Guangdong Cities (2015–2019)

Over the five-year study period (2015–2019), the mean weekly number of dengue cases across the six selected cities was 7 ± 23. The weekly average ambient temperature and relative humidity were 22.44 ± 5.13 °C and 78.95 ± 8.68%, respectively. Detailed descriptive statistics are summarized in Table 1. The weekly time-series trends over the 2015–2019 period are depicted in Figure S2.

Table 1. Descriptive statistics of weekly dengue cases and meteorological factors across six cities in Guangdong Province during 2015–2019.

Variable	Mean	SD *	Min *	P25 *	Median	P75 *	Max *
Dengue cases	7	23	0	0	0	2	462
Temperature (°C)	22.44	5.13	6.45	18.07	23.53	26.99	31.12
Relative humidity (%)	78.95	8.68	32.26	74.44	80.96	85.09	95.15

* SD, standard deviation; Min, minimum; P25, 25th percentile; P75, 75th percentile; Max, maximum.

3.2. Exposure-Response Relationships of Meteorological Factors and The Week of The Year with Dengue Incidence Risk

Based on the 2016–2019 training dataset, Figure 1 illustrates the exposure-response curves of the week of the year, 6-week moving average (Lag 0–6) temperature, and relative humidity on dengue incidence risk across the six cities. The association between temperature and this risk exhibited an inverted U-shaped pattern, with the relative risk peaking at exactly 20.2 °C. Furthermore, relative humidity demonstrated an overall positive

correlation with the incidence risk. Similarly, the relationship between the week of the year and dengue incidence risk also followed an inverted U-shaped curve, reaching its maximum risk period between weeks 38 and 40.

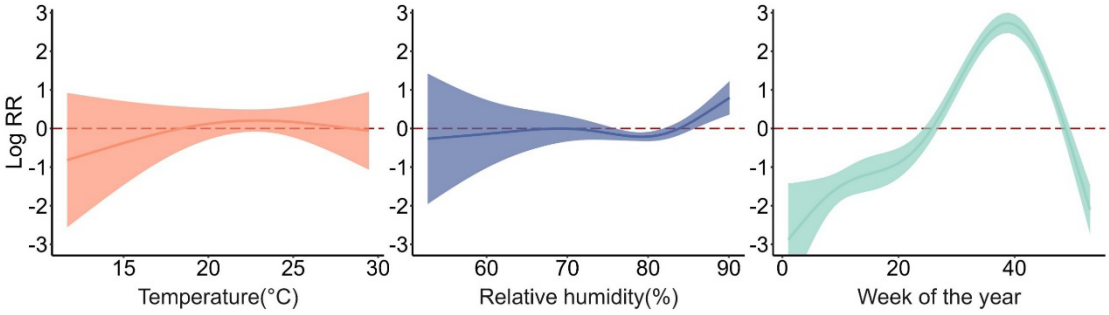

Figure 1. Exposure-response curves of week of the year, 6-week moving average temperature, and relative humidity with dengue incidence risk across six cities in Guangdong Province during 2016–2019.

3.3. Feature Weights Derived from the Random Forest Model

Utilizing the Random Forest model, the Increase in Node Purity metrics for the week of the year, 6-week moving average temperature, and relative humidity on dengue cases were evaluated at 111,276.1, 147,885.7, and 141,406.9, respectively, yielding relative weights of 0.28, 0.37 and 0.35 (Figure 2).

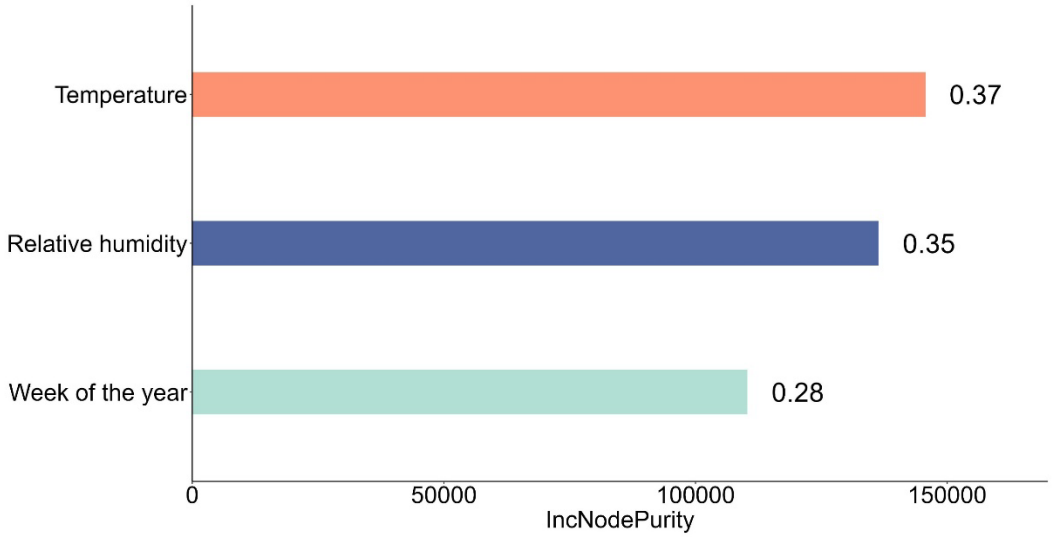

Figure 2. The Increase in Node Purity (IncNodePurity) and corresponding relative weights of the week of the year, Lag 0–6 temperature, and relative humidity regarding dengue incidence across six cities.

3.4. Characteristics of the Dengue Meteorological Risk Index (DMRI)

The weekly DMRI was calculated for the six cities in Guangdong Province. During the 2015–2019 period, the mean weekly DMRI across these cities was 51.49 ± 26.78, with a median of 48.75 (interquartile range [IQR]: 30.68–76.88). This overall distribution is illustrated in Figure 3, and the corresponding time-series trends of the mean weekly DMRI are presented in Figure S3. The mean weekly DMRI values for 2015 and the 2016–2019 period were 50.37 ± 26.82 and 51.78 ± 26.77, respectively, with detailed distributions provided in Table S4 and Figure S4.

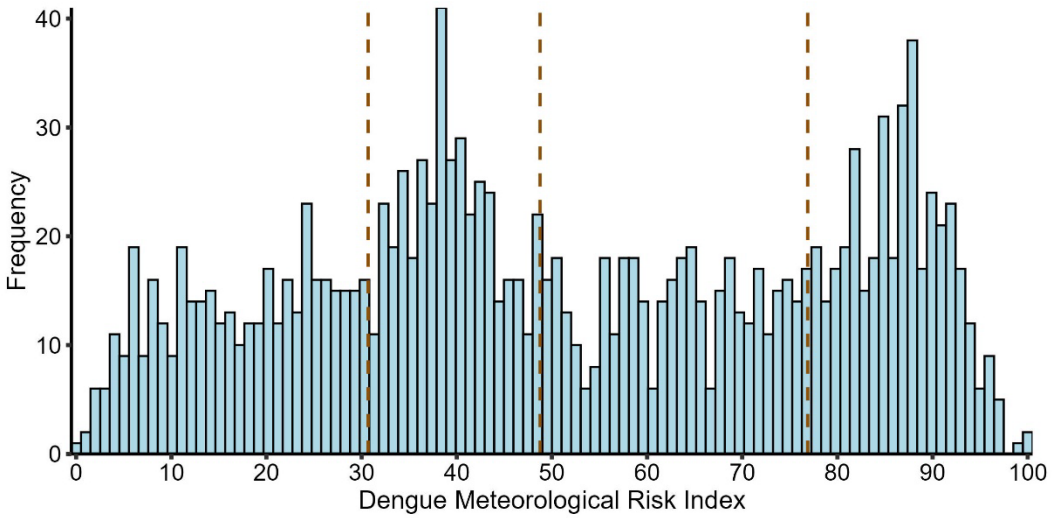

Figure 3. Distribution of the Dengue Meteorological Risk Index (DMRI) across six cities during 2015–2019. (Vertical dashed lines indicate the 25th, 50th, and 75th percentiles).

3.5. Validation and Risk Stratification of the DMRI

We further applied a GAMM to the 2016–2019 dataset to quantify the association between the DMRI and dengue cases. The findings demonstrated a linear positive relationship, with dengue incidence risk rising proportionally as the index increased (Figure 4). On average, a 1-unit increment in the DMRI contributed to an 8.82% (95% CI: 6.33%, 11.37%) increase in dengue incidence risk.

According to the mean and standard deviation (Table S5), dengue risk was categorized into four tiers: low, moderate, moderately high, and high. Internal validation using the 2016–2019 data showed that out of the total weeks, 354, 418, 175, and 301 weeks fell into the low, moderate, moderately high, and high-risk categories, yielding mean case counts of 0.27, 1.19, 5.86, and 23.30, respectively. External validation with the 2015 data confirmed this trend, with 94, 114, 44, and 66 weeks distributed across the four respective levels, recording mean case counts of 0.20, 0.34, 1.30, and 22.48 (Table 2).

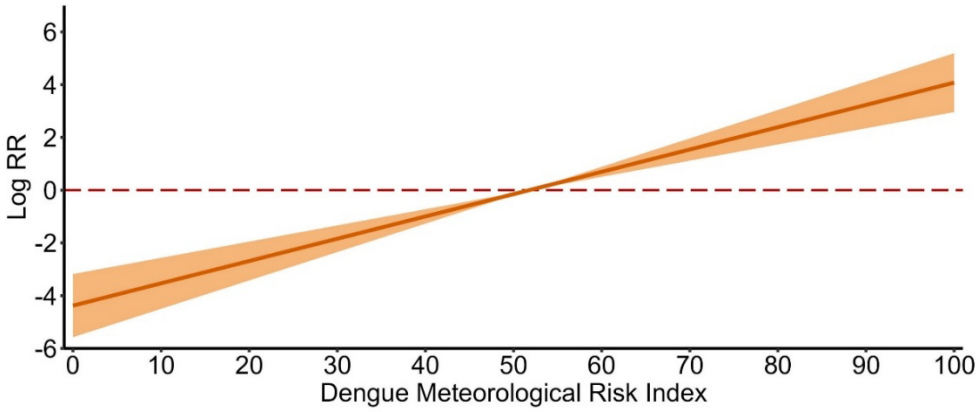

Figure 4. Exposure-response curves of DMRI with dengue incidence risk across six cities in Guangdong Province during 2016–2019.

Table 2. Dengue risk stratification and corresponding case counts across six cities in Guangdong Province during the training (2016–2019) and validation (2015) periods.

Periods	Low Risk	Moderate Risk	Moderately High Risk	High Risk
Training period	0.27 (94/354)	1.19 (498/418)	5.86 (1026/175)	23.30 (7013/301)
2016	0.23 (21/91)	0.36 (38/105)	1.42 (64/45)	5.21 (370/71)
2017	0.18 (17/96)	0.46 (42/92)	3.37 (155/46)	15.05 (1174/78)
2018	0.13 (11/85)	1.11 (127/114)	5.80 (232/40)	28.64 (2091/73)
2019	0.55 (45/82)	2.72 (291/107)	13.07 (575/44)	42.76 (3378/79)
Validation period	0.20 (19/94)	0.34 (39/114)	1.30 (57/44)	22.48 (1484/66)

3.6. Sensitivity Analysis

The sensitivity analyses showed that our findings were robust when modifying the degrees of freedom (df) for meteorological variables in the baseline GAMM, adjusting the df for the time variable, varying the df for the DMRI in the final association GAMM and altering the moving average lag periods for temperature and relative humidity (Figure S5–S8). Furthermore, the comparison of alternative weighting schemes confirmed the advantage of our data-driven approach: the GAMM incorporating the RF-weighted DMRI exhibited stronger explanatory power ($R_m^2 = 0.17, R_c^2 = 0.38$) than the model using an equal-weight DMRI ($R_m^2 = 0.13, R_c^2 = 0.31$) (Table S6).

4. Discussion

Based on surveillance data and high-resolution meteorological reanalysis datasets from high-incidence cities in Guangdong Province, this study developed a Dengue Meteorological Risk Index (DMRI) by integrating Generalized Additive Mixed Models (GAMMs) with the Random Forest algorithm. This index enables the quantification of comprehensive dengue risk under complex meteorological conditions. Our findings demonstrate that the DMRI can robustly identify high-risk window periods for dengue transmission, exhibiting excellent discriminatory capacity in both internal and external validations, thereby providing a solid scientific foundation for dengue prevention and control.

In this study, we confirmed an inverted U-shaped relationship between ambient temperature and dengue incidence risk. This finding aligns with a well-established body of literature demonstrating that dengue transmission peaks within an optimal temperature range and attenuates under extreme thermal conditions [9,23,24]. For instance, Mailepessov et al. [24] conducted a time-series analysis in Singapore and reported that dengue risk peaked at 28–29 °C, declining at temperatures above or below this threshold. This phenomenon possesses strong biological plausibility. Optimal temperatures enhance transmission efficiency by accelerating mosquito development, increasing biting frequency, and shortening the viral Extrinsic Incubation Period (EIP) [25,26]. Conversely, excessive heat suppresses risk by increasing vector mortality and depleting breeding habitats via evaporation [27]. Rather than presenting this established ecological relationship as a primary novel discovery, our study views it as a crucial, context-specific validation step. Notably, the peak dengue risk in our study was observed at approximately 20.2 °C, which is lower than the biological optimum reported in laboratory settings. This discrepancy may be partially attributable to vector ecology, human behavior, and epidemiological dynamics. First, from an ecological standpoint, the dominant vector in our study region is *Aedes albopictus*, which exhibits greater cold tolerance and a slightly lower thermal optimum for survival and transmission compared to the strictly tropical *Aedes aegypti* [28]. Second, human behavioral patterns significantly modulate exposure risk. Extreme summer heat (>30 °C) frequently drives local populations indoors into air-conditioned environments, inadvertently reducing human-vector contact. Conversely, milder temperatures around 20–25 °C encourage outdoor recreational activities [29], thereby amplifying exposure to exophagic (outdoor-biting) mosquitoes. Furthermore, the lag structure contributes to this shift. Local dengue outbreaks typically peak in autumn when temperatures decline. Our 0–6 week moving average captures cases generated during earlier, warmer periods, statistically aligning the highest incidence risk with these cooler autumn temperatures. Finally, while the ERA5-Land dataset provides gridded estimates, these city-averaged temperatures may underestimate the actual, warmer conditions of sheltered urban microclimates where mosquitoes breed.

We observed a generally positive correlation between relative humidity and dengue risk, consistent with previous findings [30–32]. For instance, Xu et al. [33] demonstrated that elevated relative humidity may serve as a crucial driver of secondary seasonal dengue peaks in the Philippines. The underlying mechanisms through which humidity influences dengue transmission are hypothesized to operate via several pathways. High-humidity environments effectively prevent adult mosquitoes from desiccation, thereby reducing mortality and extending vector lifespan [34]. Additionally, *Aedes* mosquitoes exhibit peak blood-feeding and oviposition activity at relative humidity levels of 70–80%, which is notably the standard humidity range employed in most laboratory-based mosquito experiments [35]. Humidity also frequently serves as a proxy indicator for precipitation. High humidity is often accompanied by rainfall, which expands water-filled microhabitats such as tree holes, discarded containers, and tires, thereby providing abundant breeding sites for larvae [36]. Supporting this notion, Polwiang [37] analyzed dengue surveillance data from Bangkok, Thailand (2003–2017) and reported that each 1% increase in rainfall corresponded to a 3.3% rise in dengue incidence.

In constructing the DMRI, we incorporated the exposure-response relationship between the week of the year and dengue incidence risk. This inclusion was motivated by the pronounced long-term seasonality of dengue epidemics, a pattern not fully explained by temperature and humidity alone. As a comprehensive temporal metric, the week of the year captures unmeasured socio-ecological periodicities, including seasonal population mobility

(e.g., summer vacations and school reopening), shifts in outdoor behavioral patterns, and the cyclical implementation of vector control measures [38–41]. The Random Forest model in present study assigned a weight of 0.28 to the week of the year, highlighting its importance as a key indicator of dengue risk. Our analysis revealed an inverted U-shaped association between the week of the year and dengue incidence risk, with risk peaking between weeks 38 and 40 (late September to early October). This pattern closely aligns with the epidemiological characteristics of Guangdong Province [6]. Incorporating the week of the year into the DMRI thus serves as a form of baseline calibration that reflects local transmission dynamics. By leveraging temporal inertia to constrain the explanatory contribution of meteorological variables, this approach effectively minimizes spurious high-risk alerts during non-epidemic periods (e.g., a sudden temperature surge in warm winter weeks), thereby enhancing both the robustness and specificity of the DMRI in real-world applications.

Compared to existing dengue risk assessment frameworks [13,42,43], the proposed DMRI offers distinct practical advancements, particularly in bridging the gap between meteorological data and actionable public health decisions. While many existing early-warning systems rely on parameterized statistical approach (e.g., DLNM) or multi-dimensional datasets (e.g., real-time mobility and socio-economic variables) that require specialized analytical skills, the DMRI synthesizes multifaceted meteorological risks into a single, intuitive metric. Conceptually similar to the Air Quality Health Index (AQHI) [44], this streamlined design significantly improves interpretability and facilitates timely risk communication among meteorologists, policymakers, and the public. In practice, local health departments (e.g., Centers for Disease Control and Prevention, CDCs) can seamlessly operationalize the DMRI into routine surveillance systems without specialized statistical software or advanced analytical expertise. The calculation requires only two universally accessible inputs, namely weekly mean temperature and relative humidity, both obtainable from standard meteorological stations or publicly available reanalysis datasets. Following the pre-established exposure-response curves and weighting coefficients provided in this study, the weekly DMRI can be computed using basic spreadsheet software, enabling rapid, low-cost integration into existing public health workflows. Furthermore, by coupling the DMRI calculation with short-term weather forecasts (1- to 2-week-ahead), public health agencies can achieve genuine proactive early warning capabilities without the data-gathering delays inherent in complex models.

The ultimate objective of developing a risk index is to guide practical public health interventions. In this study, the DMRI was standardized to a 0–100 scale and stratified into four tiers based on statistical distributions. When the index exceeds these predefined thresholds, it can guide adaptive resource allocation for local health authorities alongside public prevention guidelines: (1) Low-risk period: While external risk remains generally low, health departments should maintain baseline vector surveillance. The public is encouraged to maintain routine environmental sanitation and regularly clear stagnant water. (2) Moderate-risk period: As transmission risk may begin to rise, interventions should shift toward preventing local transmission from imported cases. Health agencies could initiate public awareness campaigns, while individuals should ensure window screen integrity and use repellents in vector-dense areas. (3) Moderately high-risk period: Elevated outdoor adult mosquito density may pose a substantial biting risk. Health authorities should intensify active vector monitoring and pre-allocate hospital screening resources. The public is advised to minimize prolonged stays in shaded areas during peak Aedes activity hours (dawn and dusk) and seek immediate medical screening for dengue-like symptoms. (4) High-risk period: As this level suggests an elevated risk of community transmission, intensified intervention strategies become essential. Public health departments must deploy targeted adulticide fogging, conduct active epidemiological tracing, and mobilize community-based source reduction. Simultaneously, confirmed cases must strictly adhere to isolation protocols to prevent secondary local transmission.

Despite the robust performance of the DMRI, several limitations should be acknowledged. First, the index is primarily driven by mean temperature and relative humidity. Other meteorological elements (e.g., rainfall, wind speed), environmental factors (e.g., air pollution), and complex socio-ecological dynamics (e.g., imported cases, population mobility, and reactive vector control) [45–47] were omitted. Although we mitigated unmeasured temporal confounding and spatial heterogeneity via our modeling framework, dynamic socio-demographic indicators were not explicitly parameterized. Second, we adopted an additive framework using Random Forest (RF) variable importance for weighting. While practical, this approach presents methodological limitations. RF importance metrics can be sensitive to collinearity between predictors like temperature and humidity, meaning the weights serve as an empirical approximation rather than strict causal estimates. Furthermore, the additive design does not explicitly capture synergistic interaction effects (e.g., temperature and humidity, air pollution and meteorology) [48], potentially leading to an incomplete representation of extreme joint meteorological effects. Third, data constraints restricted the complexity of our lag structure modeling. Applying parameter-intensive frameworks like DLNM to our limited weekly aggregated data risks severe overfitting. Consequently, we utilized a simple moving average (Lag 0–6) to maintain model stability. While this straightforward approach aligns with

our goal of developing an easily calculable index, it might slightly attenuate specific delayed peak effects compared to more complex multi-dimensional lag surfaces. Finally, our reliance on macro-level, weekly aggregated data precludes the analysis of daily meteorological extremes. Future iterations should integrate high-resolution, multi-source data and direct entomological evidence to further refine this unified early warning index.

In conclusion, this study developed the Dengue Meteorological Risk Index (DMRI) by quantifying the ecological associations between meteorological drivers, temporal patterns (week of the year), and dengue risk in Guangdong Province. As an accessible and intuitive tool, the DMRI has the potential to act as a supplementary indicator to support local health authorities in early warning and inform public prevention guidelines. However, given its basis in ecological associations, the index should not be viewed as a standalone forecasting tool. While this analytical framework may offer a methodological reference for other endemic regions, its application to different geographical settings would necessitate context-specific validation.

Supplementary Materials

The additional data and information can be downloaded at: https://media.sciltp.com/articles/others/260623152402683 7/ECDD-26030104-SI.pdf. Table S1: Number of dengue cases in 21 prefecture-level cities of Guangdong Province, 2015–2019. Table S2: Correlation matrix of weekly dengue cases, meteorological factors, and time-related variables. Table S3: Variance Inflation Factors (VIF) for the 0–6 week moving average temperature, 0–6 week moving average relative humidity, and week of the year. Table S4: Descriptive statistics of weekly dengue cases and meteorological factors across six cities in Guangdong Province during 2015–2019. Table S5: Descriptive statistics of the Dengue Meteorological Risk Index (DMRI) across the six cities in Guangdong Province during 2015–2019. Table S6: Comparison of model performance between the RF-weighted DMRI and equal-weight DMRI. Figure S1: Spatial distribution of dengue cases in Guangdong Province, 2015–2019. (Note: Cities in bold were selected for subsequent modeling analysis). Figure S2: Weekly number of dengue cases in 6 cities of Guangdong Province, 2015–2019. Figure S3: Weekly Dengue Meteorological Risk Index (DMRI) in 6 cities of Guangdong Province, 2015–2019. Figure S4: Distribution of the Dengue Meteorological Risk Index (DMRI) across six cities during the validation (2015) and training (2016–2019) periods. (Vertical dashed lines indicate the 25th, 50th, and 75th percentiles). Figure S5: Sensitivity analysis varying the degrees of freedom (df = 3–6) for temperature and relative humidity. Figure S6: Sensitivity analysis varying the degrees of freedom (df = 5–7) for week of year variable. Figure S7: Sensitivity analysis varying the degrees of freedom (df = 3–6) for Dengue Meteorological Risk Index. Figure S8: Sensitivity analysis varying moving average lag periods for temperature and relative humidity.

Author Contributions

J.H. and L.L. contributed equally and are joint first authors. J.H.: methodology, software, writing—original draft preparation; L.L.: data curation, writing—original draft preparation; H.C.: data curation, validation; Q.F.: data curation, validation; D.W.: data curation, visualization; G.H.: software, validation; T.L.: validation; F.Z.: visualization; F.J.: data curation; Z.L.: software; F.L.: supervision; X.L.: methodology; M.K.: supervision, writing—reviewing and editing; W.M.: conceptualization, supervision, writing—reviewing and editing. All authors have read and agreed to the published version of the manuscript.

Funding

This study was funded by the National Key Research and Development Program of China (2026ZD01909500); Health Talents Project of Guangdong Special Support Program (0820250120); National Natural Science Foundation of China (42475183).

Institutional Review Board Statement

The study was conducted according to the guidelines of the Declaration of Helsinki, and approved by the Medical Ethics Committee of Jinan University (protocol code: JNU-20260320-001, date of approval: 2026-03-20).

Informed Consent Statement

Patient consent was waived because dengue fever is a notifiable infectious disease. In addition, only statistical data were used in the analysis, and no personally identifiable information was involved.

Data Availability Statement

Infectious disease data cannot be shared publicly due to legal and privacy restrictions. The raw meteorological data are publicly available from the ERA5-Land dataset (ECMWF). The analytical code used to generate the findings of this study will be provided by the corresponding author (mawj@gdiph.org.cn, W.M.) upon reasonable request.

Conflicts of Interest

The authors declare no conflict of interest.

Use of AI and AI-Assisted Technologies

No AI tools were utilized for this paper.

References

1. Kularatne, S.A. Dengue fever. *BMJ* **2015**, *351*, h4661.
2. Aguiar, M.; Anam, V.; Blyuss, K.B.; et al. Mathematical models for dengue fever epidemiology: A 10-year systematic review. *Phys. Life Rev.* **2022**, *40*, 65–92.
3. Harish, V.; Colón-González, F.J.; Moreira, F.R.R.; et al. Human movement and environmental barriers shape the emergence of dengue. *Nat. Commun.* **2024**, *15*, 4205.
4. Islam, J.; Frentiu, F.D.; Devine, G.J.; et al. A state-of-the-art review of long-term predictions of climate change impacts on dengue transmission risk. *Environ. Health Perspect.* **2025**, *133*, 56002.
5. Deng, J.; Zhang, H.; Wang, Y.; et al. Global, regional, and national burden of dengue infection in children and adolescents: An analysis of the Global Burden of Disease Study 2021. *EClinicalMedicine* **2024**, *78*, 102943.
6. Cui, F.; He, F.; Huang, X.; et al. Dengue and dengue virus in Guangdong, China, 1978–2017: Epidemiology, seroprevalence, evolution, and policies. *Front. Med.* **2022**, *9*, 797674.
7. Anikeeva, O.; Hansen, A.; Varghese, B.; et al. The impact of increasing temperatures due to climate change on infectious diseases. *BMJ* **2024**, *387*, e079343.
8. Zheng, L.; Ren, H.-Y.; Shi, R.-H.; et al. Spatiotemporal characteristics and primary influencing factors of typical dengue fever epidemics in China. *Infect. Dis. Poverty* **2019**, *8*, 24.
9. Wang, Y.; Wei, Y.; Li, K.; et al. Impact of extreme weather on dengue fever infection in four Asian countries: A modelling analysis. *Environ. Int.* **2022**, *169*, 107518.
10. Liu, Z.; Zhang, Q.; Li, L.; et al. The effect of temperature on dengue virus transmission by Aedes mosquitoes. *Front. Cell. Infect. Microbiol.* **2023**, *13*, 1242173.
11. Pinontoan, O.R.; Sumampouw, O.J.; Ticoalu, J.H.V.; et al. The variability of temperature, rainfall, humidity and prevalance of dengue fever in Manado City. *Bali Medical Journal* **2022**, *11*, 2722.
12. Polrob, W.; La-up, A. Nonlinear and lagged effects of climate variability on dengue incidence in an urban megacity: A distributed lag non-linear model (DLNM) based study in Bangkok, Thailand. *BMC Public Health* **2025**, *25*, 4024.
13. Belau, M.H.; Boenecke, J.; Ströbele, J.; et al. Integrated rapid risk assessment for dengue fever in settings with limited diagnostic capacity and uncertain exposure: Development of a methodological framework for Tanzania. *PLoS Negl. Trop. Dis.* **2025**, *19*, e0012946.
14. Li, Z.; Xu, R.; Huang, W.; et al. Developing a community-specific daily weather health risk index across Australia using explainable machine learning. *Environ. Sci. Technol.* **2025**, *59*, 24268–24278.
15. Kumharn, W.; Piwngam, W.; Pilahome, O.; et al. Effects of meteorological factors on dengue incidence in Bangkok city: A model for dengue prediction. *Model. Earth Syst. Environ.* **2023**, *9*, 1215–1222.
16. Muñoz-Sabater, J.; Dutra, E.; Agustí-Panareda, A.; et al. ERA5-Land: A state-of-the-art global reanalysis dataset for land applications. *Earth Syst. Sci. Data* **2021**, *13*, 4349–4383.
17. Mateus, P.; Mendes, V.B.; Plecha, S.M. HGPT2: An ERA5-based global model to estimate relative humidity. *Remote Sens.* **2021**, *13*, 2179.
18. Cabrera, M.; Taylor, G. Modelling spatio-temporal data of dengue fever using generalized additive mixed models. *Spat. Spatio-Temporal Epidemiol.* **2019**, *28*, 20–37.
19. Li, C.; Wang, X.; Wu, X.; et al. Modeling and projection of dengue fever cases in Guangzhou based on variation of weather factors. *Sci. Total Environ.* **2017**, *605*, 867–873.
20. Liu, X.; Song, M.; Tao, D.; et al. Random forest construction with robust semisupervised node splitting. *IEEE Trans. Image Process.* **2014**, *23*, 471–483.
21. Rothman, K.J.; Greenland, S.; Lash, T.L. *Modern Epidemiology*, 3rd ed.; Lippincott Williams & Wilkins: Philadelphia, Philadelphia, PA, USA, 2008.

22. Jue, L.W.L.; Min, L.; Yu, W.; Hui, H.; Lei, Z.; Yadong, W. Study on the construction of risk assessment index system of imported infectious diseases. *Chin. J. Emerg. Resusc. Disaster Med.* **2021**, *16*, 465–469.
23. Seposo, X.; Valenzuela, S.; Apostol, G.L. Socio-economic factors and its influence on the association between temperature and dengue incidence in 61 Provinces of the Philippines, 2010–2019. *PLoS Negl. Trop. Dis.* **2023**, *17*, e0011700.
24. Mailepessov, D.; Ong, J.; Aik, J. Influence of air pollution and climate variability on dengue in Singapore: A time-series analysis. *Sci. Rep.* **2025**, *15*, 13467.
25. Ebi, K.L.; Nealon, J. Dengue in a changing climate. *Environ. Res.* **2016**, *151*, 115–123.
26. Chan, M.; Johansson, M.A. The incubation periods of dengue viruses. *PLoS ONE* **2012**, *7*, e50972.
27. Carrington, L.B.; Armijos, M.V.; Lambrechts, L.; et al. Effects of fluctuating daily temperatures at critical thermal extremes on *Aedes aegypti* life-history traits. *PLoS ONE* **2013**, *8*, e58824.
28. Doeurk, B.; Leng, S.; Long, Z.; et al. Impact of temperature on survival, development and longevity of *Aedes aegypti* and *Aedes albopictus* (Diptera: Culicidae) in Phnom Penh, Cambodia. *Parasit. Vectors* **2025**, *18*, 362.
29. Fan, Y.; Wang, J.; Obradovich, N.; et al. Intraday adaptation to extreme temperatures in outdoor activity. *Sci. Rep.* **2023**, *13*, 473.
30. Lu, L.; Lin, H.; Tian, L.; et al. Time series analysis of dengue fever and weather in Guangzhou, China. *BMC Public Health* **2009**, *9*, 395.
31. Wu, X.; Lang, L.; Ma, W.; et al. Non-linear effects of mean temperature and relative humidity on dengue incidence in Guangzhou, China. *Sci. Total Environ.* **2018**, *628*, 766–771.
32. Noureldin, E.; Shaffer, L. Role of climatic factors in the incidence of dengue in Port Sudan City, Sudan. *East. Mediterr. Health J.* **2019**, *25*, 852–860.
33. Xu, Z.; Bambrick, H.; Yakob, L.; et al. High relative humidity might trigger the occurrence of the second seasonal peak of dengue in the Philippines. *Sci. Total Environ.* **2020**, *708*, 134849.
34. Lucio, P.S.; Degallier, N.; Servain, J.; et al. A case study of the influence of local weather on *Aedes aegypti* (L.) aging and mortality. *J. Vector Ecol.* **2013**, *38*, 20–37.
35. Dong, L.; Bradford, E.F.; Barnett, J.M.; et al. Post-biting behavioral reprogramming underlies reproductive efficiency in *Aedes aegypti* mosquitoes. *Cell Reports* **2025**, *44*, 116663.
36. Zahouli, J.B.; Koudou, B.G.; Müller, P.; et al. Urbanization is a main driver for the larval ecology of Aedes mosquitoes in arbovirus-endemic settings in south-eastern Côte d'Ivoire. *PLoS Negl. Trop. Dis.* **2017**, *11*, e0005751.
37. Polwiang, S. The time series seasonal patterns of dengue fever and associated weather variables in Bangkok (2003–2017). *BMC Infect. Dis.* **2020**, *20*, 208.
38. Buckee, C.O.; Tatem, A.J.; Metcalf, C.J.E. Seasonal population movements and the surveillance and control of infectious diseases. *Trends Parasitol.* **2017**, *33*, 10–20.
39. Chandren, J.R.; Wong, L.P.; Abubakar, S. Practices of dengue fever prevention and the associated factors among the Orang Asli in Peninsular Malaysia. *PLoS Negl. Trop. Dis.* **2015**, *9*, e0003954.
40. Nguyen-Tien, T.; Do, D.C.; Le, X.L.; et al. Risk factors of dengue fever in an urban area in Vietnam: A case-control study. *BMC Public Health* **2021**, *21*, 664.
41. Wen, T.-H.; Lin, M.-H.; Teng, H.-J.; et al. Incorporating the human-Aedes mosquito interactions into measuring the spatial risk of urban dengue fever. *Appl. Geogr.* **2015**, *62*, 256–266.
42. Singh, G.; Mitra, A.; Soman, B. Development and use of a reproducible framework for spatiotemporal climatic risk assessment and its association with decadal trend of dengue in India. *Indian J. Community Med.* **2022**, *47*, 50–54.
43. Leung, X.Y.; Islam, R.M.; Adhami, M.; et al. A systematic review of dengue outbreak prediction models: Current scenario and future directions. *PLoS Negl. Trop. Dis.* **2023**, *17*, e0010631.
44. Chen, M.J.; Guo, Y.L.; Lin, P.; et al. Air quality health index (AQHI) based on multiple air pollutants and mortality risks in Taiwan: Construction and validation. *Environ. Res.* **2023**, *231*, 116214.
45. Gao, P.; Pilot, E.; Rehbock, C.; et al. Land use and land cover change and its impacts on dengue dynamics in China: A systematic review. *PLoS Negl. Trop. Dis.* **2021**, *15*, e0009879.
46. Telle, O.; Grandadam, M.; Philippon, D.; et al. Dengue dynamics beyond biological factors: Revealing the nexus between urbanization planning, and mobilities in Vientiane, Lao PDR. *PLoS Negl. Trop. Dis.* **2025**, *19*, e0011990.
47. Nakase, T.; Giovannetti, M.; Obolski, U.; et al. Population at risk of dengue virus transmission has increased due to coupled climate factors and population growth. *Commun. Earth Environ.* **2024**, *5*, 475.
48. Ju, X.; Zhang, W.; Yimaer, W.; et al. How air pollution altered the association of meteorological exposures and the incidence of dengue fever. *Environ. Res. Letters* **2022**, *17*, 124041.